= 138 Hz, P^c), -32.6 (d, 2 P, ^3J(PP) = 138 Hz, P^a); ^{13}C (at -80 °C), δ 207.3 (s, CO). A limiting low-temperature ^{1}H NMR spectrum was not obtained at -90 °C, and the resonances were too broad to be useful.

[Ni₃(μ_3-CO)(μ-dmpm)₄][PF₆]₂. To a solution of [Ni₃(μ_3-CO)(μ-dmpm)₄][Na(BH₃CN)₃] (0.3 g) in acetone (10 mL) was added excess NH₄PF₆ (0.2 g) in ethanol (8 mL). After 5 min, pentane (20 mL) was added to precipitate the product as a purple solid, which was washed with ether and pentane and dried under vacuum: yield 90%; mp 303-306 °C. Anal. Calcd for C₂₁H₅₆F₁₂Ni₃OP₁₀: C, 24.3; H, 5.4. Found: C, 23.9; H, 5.5. The NMR data for the cation were the same as for **1a**. IR: ν(CO) 1694 cm⁻¹; ν(^{13}CO) = 1645.5 cm⁻¹ (obtained as a Nujol mull from a sample enriched in ^{13}CO).

X-ray Analysis of [Ni₃(μ_3-CO)(μ-dmpm)₄][Na(BH₃CN)₃]. A crystal, grown as described above from ethanol/ether and having dimensions 0.50 × 0.50 × 0.60 mm, was mounted on a glass fiber for data collection in an Enraf-Nonius CAD4 diffractometer. The cell data and orientation matrix were determined from the setting angles of 25 reflections in the range 10° < θ < 14°. From the systematic absences (h0l, h + l = 2n; 0k0, k = 2n) and from the subsequent least-squares refinement, the monoclinic space group was determined to be P2₁/n (No. 14): a = 12.606 (5) Å, b = 24.113 (7) Å, c = 14.469 (4) Å, β = 95.99 (3)°, V = 4374 (5) Å³, Z = 4, D_c = 1.35 g cm⁻³, F(000) = 1872, Mo Kα radiation (λ = 0.710 73 Å), μ(Mo Kα) = 16.1 cm⁻¹. Intensity data (9952 reflections, 9524 unique reflections) were measured at 21 °C with use of the ω-2θ

scan technique to a maximum of 2θ = 40.0°; Lorentz, polarization, decay (7.7% over the data collection), and an empirical absorption correction were applied to the data. The structure was solved with the aid of MULTAN, which gave the positions of the three nickel atoms and six phosphorus atoms. Full-matrix least-squares refinement, with hydrogens allowed as riding atoms, gave R_1 = 0.029 and R_2 = 0.038 for 6563 reflections with I ≥ 3σ(I). A final difference map revealed no chemically significant features. Scattering factors[10] and anomalous dispersion effects[11] were taken from the literature. All calculations were performed on a PDP-11 computer using SDP-PLUS.[12]

Supplementary Material Available: Tables of experimental details, general temperature factors, calculated hydrogen coordinates, least-squares planes, and torsion angles (14 pages); a table of observed and calculated structure factors (66 pages). Ordering information is given on any current masthead page.

(10) Cromer, D. T.; Waber, J. T. *International Tables for X-ray Crystallography*; Kynoch Press: Birmingham, England, 1974; Vol. 4, Tables 2.2B and 2.3.1.

(11) Ibers, J. A.; Hamilton, W. C. *Acta Crystallogr.* **1974**, *17*, 781.

(12) Frenz, B. A. In *Computing in Crystallography*; Schenk, H.; Olthof-Hazelkamp, R., van Konigsveld, H., Bassi, G. C., Eds.; Delft University Press: Delft, Holland, 1978; p 64.

Synthesis, Structure, and Fluxionality of Clusters Formed by Addition of Bidentate Ligands to [Pt₃(μ_3-CO)(μ-dppm)₃]²⁺ (dppm = Ph₂PCH₂PPh₂): Structure of [Pt₃(μ-CO)(μ-dppm)₃(μ-S₂CNMe₂)][PF₆]

Arleen M. Bradford and Richard J. Puddephatt*

Department of Chemistry, University of Western Ontario, London, Ontario, Canada N6A 5B7

Graeme Douglas, Ljubica Manojlović-Muir, and Kenneth W. Muir

Chemistry Department, University of Glasgow, Glasgow, Scotland G12 8QQ

The 42-electron cluster cation [Pt₃(μ_3-CO)(μ-dppm)₃]²⁺ (1) reacts with bidentate ligands LL = R₂NCS₂⁻ to give [Pt₃(μ-CO)(μ-dppm)₃(μ-R₂NCS₂)]⁺ (**3a**, R = Me; **3b**, R = Et), with LL = R₃PCS₂ to give [Pt₃(μ-CO)(μ-dppm)₃(μ-R₃PCS₂)]²⁺ (**3c**, R = Et; **3d**, R = cyclohexyl), and with LL = R₂PCH₂PR₂ to give [Pt₃(μ-CO)(μ-dppm)₃(μ-R₂PCH₂PR₂)]²⁺ (**3e**, R = Me; **3f**, R = Ph). Complex **3a** has been shown by crystal structure analysis to contain the latitudinal Pt₃(μ-dppm)₃ core also present in 1. However, the carbonyl ligand has slipped from a symmetrical μ_3-bonding mode found in 1 and now approximately doubly bridges the two platinum atoms that are also bridged by the dithiocarbamate ligand. The complexes **3a-d** and **3f** exhibit fluxionality of the added ligand LL, as shown by NMR spectroscopy.

Introduction

It has been established that monodentate phosphorus- and sulfur-containing ligands react readily with the coordinatively unsaturated, 42-electron cluster complex [Pt₃(μ_3-CO)(μ-dppm)₃]²⁺ (1)[1] to give 44-electron adducts such as [Pt₃(μ_3-CO)(μ-dppm)₃(PR₃)]²⁺ and [Pt₃(SCN)(μ_3-CO)(μ-dppm)₃]⁺.[2-4] Steric hindrance appears

to prevent addition of more than one monodentate ligand except in the case of carbonyl, which can form the 46-electron complex [Pt₃(μ-CO)(CO)₂(μ-dppm)₃]²⁺.[5] The investigation of the reactions of 1 with bidentate ligands was of interest to find a more general route to unusual

(1) Ferguson, G.; Lloyd, B. R.; Puddephatt, R. J. *Organometallics* **1986**, *5*, 344.

(2) Bradford, A. M.; Jennings, M. C.; Puddephatt, R. J. *Organometallics* **1988**, *7*, 792.

(3) Bradford, A. M.; Douglas, G.; Manojlović-Muir, L.; Muir, K. W.; Puddephatt, R. J. *Organometallics* **1990**, *9*, 409.

(4) Ferguson, G.; Lloyd, B. R.; Manojlović-Muir, L.; Muir, K. W.; Puddephatt, R. J. *Inorg. Chem.* **1986**, *25*, 4190.

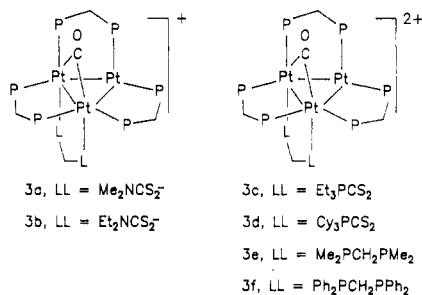(5) Lloyd, B. R.; Bradford, A. M.; Puddephatt, R. J. *Organometallics* **1987**, *6*, 424.

46-electron clusters of platinum and, in particular, to determine whether the ligands add at terminal or bridging sites, how ligand addition affects the $Pt_3(\mu_3\text{-}CO)$ linkage and metal–metal bonding, and whether fluxionality similar to that found for the complexes with monodentate ligands[2-5] would be possible. The 46-electron complex $[Pt_3(\mu\text{-}CO)(\mu\text{-}dmpm)_4][BPh_4]_2$ ($2[BPh_4]_2$; dmpm = $Me_2PCH_2PMe_2$) has been reported,[6] and a preliminary account of parts of this work has been published.[7] There are parallels between the chemistry of the Pt_3 triangle of 1 and the chemistry of similar units on a platinum metal surface.[5]

Results
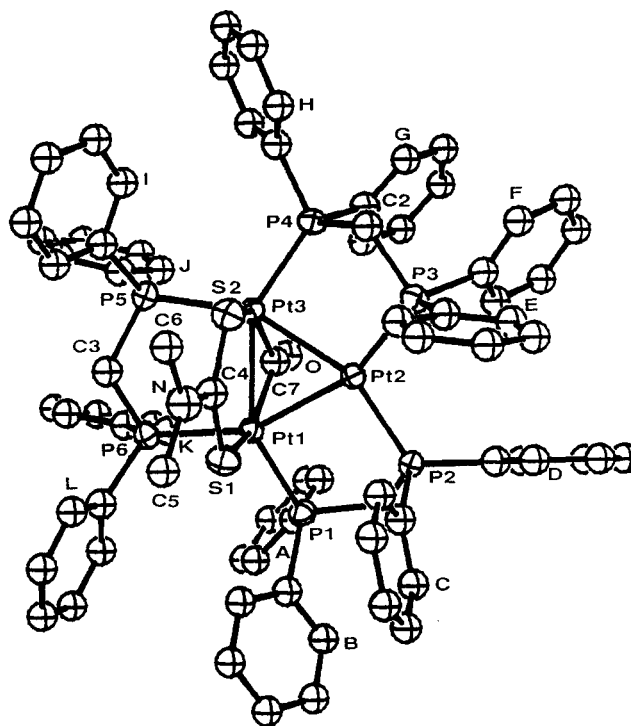
Formation of the Complexes $[Pt_3(\mu\text{-}CO)(\mu\text{-}dppm)_3L_2]^{n+}$. As monitored by ^{31}P NMR spectroscopy, the reactions of $[Pt_3(\mu_3\text{-}CO)(\mu\text{-}dppm)_3]^{2+}$ (1) with N,N-dialkyldithiocarbamate, trialkylphosphine–carbon disulfide and bis(dimethylphosphino)methane ligands gave the corresponding complexes 3a–e in at least 90% yield.

3a, LL = $Me_2NCS_2^-$
3b, LL = $Et_2NCS_2^-$
3c, LL = Et_3PCS_2
3d, LL = Cy_3PCS_2
3e, LL = $Me_2PCH_2PMe_2$
3f, LL = $Ph_2PCH_2PPh_2$

These complexes were thermally stable and could be isolated in analytically pure form as the hexafluorophosphate salts. Reaction of 1 with the bulkier ligand dppm yielded an equilibrium between 1, free dppm, and 3f. Pure 3f could be isolated as a black solid by crystallization at low temperature in the presence of excess dppm and by separation of the black crystals of 3f by hand from the red crystals of 1 that also formed. The thermodynamic parameters for the formation of 3f in acetone solution were obtained by measuring the equilibrium constant for its formation with use of ^{31}P NMR spectroscopy (see below) at temperatures from +20 to −28 °C and were $\Delta H° = -55 \pm 10$ kJ mol^{-1} and $\Delta S° = -145 \pm 50$ J K^{-1} mol^{-1}. As expected, the enthalpy term favors adduct formation while the entropy term does not. Complex 3f must be very sterically congested, and its structure would be of much interest. Unfortunately, the crystals obtained were not of diffraction quality. Instead, the structure of 3a was determined crystallographically.

Structure of $[Pt_3(\mu\text{-}CO)(\mu\text{-}dppm)_3(\mu\text{-}S_2CNMe_2)]$-$[PF_6]\cdot Me_2CO$. The complex cation contains an isosceles triangle of platinum atoms with a dppm ligand bridging each edge to form a roughly planar Pt_3P_6 latitudinal core (Figure 1). On opposite sides of the triangle, carbonyl and dimethyldithiocarbamate ligands additionally bridge the $Pt(1)-Pt(3)$ bond in a longitudinal fashion; the dihedral angles between the Pt_3 plane and those defined by the atoms $Pt(1)$, $Pt(3)$, $C(7)$, and O and by $Pt(1)$, $Pt(3)$, $S(1)$, $S(2)$, N, and $C(4)-C(6)$ are respectively 90.1 and 93.2°. The architecture of the cation thus bears a strong resemblance to that found in the dicationic cluster $[Pt_3(\mu\text{-}CO)(\mu\text{-}dmpm)_4]^{2+}$ (2; dmpm = $Me_2PCH_2PMe_2$).[6] However, in 2 all the latitudinal phosphorus atoms lie on the opposite

(6) Ling, S. S. M.; Hadj-Bagheri, N.; Manojlović-Muir, L.; Muir, K. W.; Puddephatt, R. J. *Inorg. Chem.* **1987**, *26*, 231.

(7) Bradford, A. M.; Puddephatt, R. J. *New J. Chem.* **1988**, *12*, 427.

Figure 1. View of the cluster cation $[Pt_3(\mu\text{-}CO)(\mu\text{-}dppm)_3\text{-}(S_2CNMe_2)]^+$ (3a), showing 50% probability ellipsoids. H atoms are omitted for clarity. Phenyl groups are numbered $C(X1)-C(X6)$ (X = A–L), starting at the ipso carbon atom. Only the ring identifier X is indicated, adjacent to $C(X2)$. The numbering of all non-phenyl atoms is indicated, apart from that for methylene $C(1)$, which is obscured by $C(C6)$.

side of the Pt_3 plane from the longitudinal dmpm ligand, a result attributed[6] to interligand repulsion, whereas in 3a three of the latitudinal phosphorus atoms are displaced to the same side of the Pt_3 plane as the dithiocarbamate ligand (see Table I). Also, the conformations of the Pt_2P_2C rings, regular envelopes with CH_2 flaps and near-zero $P-Pt-Pt-P$ torsion angles in 2, are less regular in 3a, as shown by the intra-ring $P-Pt-Pt-P$ torsion angles of −20.3 (1), 21.3 (1), and 4.2 (1)° across $Pt(1)-Pt(2)$, $Pt(2)-Pt(3)$, and $Pt(1)-Pt(3)$. Two of the dppm methylene carbon atoms, $C(2)$ and $C(3)$, are bent toward the dithiocarbamate ligand, which thus lies above the sterically less hindered face of the Pt_3 triangle containing only two axial phenyl rings (B and C) and four equatorial ones (E, H, I, and L).

The $Pt(2)$ center differs both sterically and electronically from the $Pt(1)$ and $Pt(3)$ centers. This difference has little influence, however, on the Pt–Pt bond lengths in that the $Pt(1)-Pt(3)$ distance of 2.622 (1) Å is only marginally longer than the effectively equal $Pt(1)-Pt(2)$ and $Pt(2)-Pt(3)$ distances of 2.612 (1) and 2.605 (1) Å. In 2 the Pt–Pt distances show a similar pattern, the bond between the more heavily substituted metal atoms being 0.024 Å longer than the mean length of the other two (see Table II). It is, however, more important to note that the mean Pt–Pt bond length in 3a (2.613 Å) is slightly shorter than the corresponding mean values of 2.634, 2.639, and 2.632 Å for the related 42-, 44-, and 46-electron clusters $[Pt_3(\mu_3\text{-}CO)(\mu\text{-}dppm)_3]^{2+}$, $[Pt_3(\mu_3\text{-}CO)(\mu\text{-}dppm)_3(P(OPh)_3)]^{2+}$, and 2.[1,3,6] Clearly, the extra four electrons in 3a, compared to the electron count for 1, do not occupy metal–metal antibonding orbitals.

The Pt–P bond lengths display greater sensitivity to their environment: the shortest involve the four-coordinate $Pt(2)$ atom, next in length are $Pt(1)-P(1)$ and $Pt(3)-P(4)$ followed by $Pt(1)-P(6)$ and $Pt(3)-P(5)$. These differences,

Table I. Selected Distances and Angles in [Pt₃(μ-CO)(μ-dppm)₃(μ-S₂CNMe₂)][PF₆] (3a[PF₆])

Bond Distances (Å)

Pt(1)-Pt(2)	2.612 (1)	Pt(1)-S(1)	2.480 (4)
Pt(1)-Pt(3)	2.622 (1)	Pt(3)-S(2)	2.503 (3)
Pt(2)-Pt(3)	2.605 (1)	Pt(1)-C(7)	2.011 (11)
Pt(1)-P(1)	2.298 (3)	P(2)...C(7)	2.671 (12)
Pt(1)-P(6)	2.356 (3)	Pt(3)-C(7)	2.023 (11)
Pt(2)-P(2)	2.246 (3)	C(7)-O	1.217 (14)
Pt(2)-P(3)	2.244 (3)	C(4)-S(1)	1.722 (11)
Pt(3)-P(4)	2.309 (3)	C(4)-S(2)	1.719 (10)
Pt(3)-P(5)	2.357 (3)	C(4)-N	1.310 (15)
P-CH₂	1.831 (11)-1.854 (12)	N-C(5)	1.473 (16)
P-C(Ph)	1.809 (12)-1.846 (8)	N-C(6)	1.456 (16)

Bond Angles (deg)

Pt(2)-Pt(1)-P(1)	94.3 (1)	Pt(2)-Pt(3)-P(4)	89.3 (1)
Pt(2)-Pt(1)-P(6)	154.5 (1)	Pt(2)-Pt(3)-P(5)	154.7 (1)
Pt(2)-Pt(1)-S(1)	89.4 (1)	Pt(2)-Pt(3)-S(2)	87.6 (1)
Pt(3)-Pt(1)-P(1)	147.0 (1)	Pt(1)-Pt(3)-P(4)	146.5 (1)
Pt(3)-Pt(1)-P(6)	95.2 (1)	Pt(1)-Pt(3)-P(5)	96.1 (1)
Pt(3)-Pt(1)-S(1)	95.0 (1)	Pt(1)-Pt(3)-S(2)	95.0 (1)
S(1)-Pt(1)-P(1)	105.4 (1)	S(2)-Pt(3)-P(4)	96.7 (1)
S(1)-Pt(1)-P(6)	88.7 (1)	S(2)-Pt(3)-P(5)	86.6 (1)
S(1)-Pt(1)-C(7)	144.2 (4)	S(2)-Pt(3)-C(7)	143.5 (4)
P(1)-Pt(1)-P(6)	110.6 (1)	P(4)-Pt(3)-P(5)	115.8 (1)
Pt(1)-Pt(2)—P(2)	94.3 (1)	Pt(3)-Pt(2)-P(3)	98.0 (1)
Pt(1)-Pt(2)-P(3)	157.3 (1)	Pt(3)-Pt(2)-P(2)	154.6 (1)
P(2)-Pt(2)-P(3)	107.3 (1)	Pt(1)-C(7)-Pt(3)	81.1 (5)
Pt(1)-C(7)-O	137.1 (8)	Pt(3)-C(7)-O	140.9 (8)
Pt(1)-S(1)-C(4)	112.6 (4)	Pt(3)-S(2)-C(4)	111.6 (4)
S(1)-C(4)-S(2)	125.3 (7)	C(4)-N-C(5)	123.3 (10)
S(1)-C(4)-N	116.5 (8)	C(4)-N-C(6)	121.5 (10)
S(2)-C(4)-N	118.1 (8)	C(5)-N-C(6)	115.1 (10)
P(1)-C(1)-P(2)	112.9 (6)	P(3)-C(2)-P(4)	109.1 (6)
P(5)-C(3)-P(6)	114.7 (6)	Pt-P-CH₂	106-111
P-P-C(Ph)	114-122	CH₂-P-C(Ph)	102-107
C(Ph)-P-C(Ph)	95-105		

Deviations (Å) from Plane Defined by Pt(1), Pt(2), and Pt(3)

P(1)	-0.842 (3)	C(1)	1.22 (1)
P(2)	0.049 (3)	C(2)	-0.54 (1)
P(3)	-0.285 (3)	C(3)	-1.06 (1)
P(4)	0.555 (3)	S(1)	-2.466 (3)
P(5)	-0.353 (3)	S(2)	-2.481 (3)
P(6)	-0.183 (3)	C(7)	1.53 (1)

which are closely paralleled by the corresponding Pt–P distances in **2**, could arise as a result of a rehybridization of Pt orbitals, due to the higher coordination numbers of Pt(1) and Pt(3), or could simply be the result of steric congestion at these sites. All the Pt–P distances in **3a** are, however, in the range expected for Pt–P bonds.

The Pt–S distances in **3a** (2.480 (4) and 2.503 (3) Å) are, on average, some 0.15 Å longer than any previously reported Pt–S(dithiocarbamate) bond length: for example, 2.331 (7) Å found for [Pt₂Cl₃(PEt₃)₂(S₂CNMe₂)],[8] where the dithiocarbamate ligand bridges two platinum centers that are not bound to each other and 2.339 (4) Å for [Pt(S₂CNEt₂)₂(PPh₃)] and 2.31 Å for [Pt(S₂CNEt₂)₂], where the dithiocarbamate ligands chelate to the platinum atom.[9] Steric factors could play a role in these lengthened Pt–S bonds. It should be noted, however, that few dithiocarbamate complexes of platinum have been structurally characterized and that none of them, apart from **3a**, contain a dithiocarbamate bridging a Pt–Pt bond. In **2**, the longitudinal Pt–P distances (2.355 (3) and 2.372 (3) Å), though at the upper end of the range typical of Pt–P(phosphine) distances, are not anomalously long; for example, they are comparable with the Pt(1)-P(6) and

(8) Goel, A. B.; Goel, S.; Van Derveer, D.; Brinkley, C. G. *Inorg. Chim. Acta* **1982**, *64*, L173.

(9) Fackler, J. P., Jr.; Thompson, L. D.; Lin, I. J. B.; Stephenson, T. A.; Gould, R. O.; Alison, J. M. C.; Fraser, A. J. F. *Inorg. Chem.* **1982**, *21*, 2397.

Table II. Selected Structural and Spectroscopic Data for Pt₃(μ-CO) Complexes[a]

	1	2	3a
Pt(1)-Pt(2)/Å	2.638 (1)	2.628 (1)	2.612 (1)
Pt(1)-Pt(3)/Å	2.650 (1)	2.648 (1)	2.622 (1)
Pt(2)-Pt(3)/Å	2.613 (1)	2.620 (1)	2.605 (1)
Pt(1)-C/Å	2.095 (9)	2.049 (8)	2.011 (11)
Pt(2)-C/Å	2.089 (8)	2.43 (1)	2.671 (12)
Pt(3)-C/Å	2.080 (9)	2.061 (9)	2.023 (11)
C-O/Å	1.154 (9)	1.194 (10)	1.217 (14)
ν(CO)/cm⁻¹ [b]	1765	1730	1736
¹J(PtC)/Hz		730	780
δ(¹³CO)/ppm[c]			207.48
ref	1	6	this work

[a] Latitudinal dppm and dmpm ligands are motted for clarity. [b] Samples run as Nujol mulls. [c] Solvent acetone-d₆.

Table III. ³¹P and ¹³C NMR and IR Data for Complexes 3a-d and 3f[a]

	3a	3b	3c	3d	3f
δ(Pᵃ,ᵇ,ᶜ)ᵇ,ᵈ	-32.1	-32.1	-26.4	-26.9	-43.2
¹J(PtPᵃ)	3280	3110	3100	3180	2900
²J(PtPᵃ)	120	135	90	100	270
³J(PP)	200	185	185	180	190
δ(Pᵈ)ᶜ			54.4	48.9	-22.1
J(PtPᵈ)			170ᵈ	166ᵈ	720ᵉ
δ(CO)	207.5		211.9	213.1	215.7
¹J(PtC)	780ᶠ		760	745	680ᵍ
ν(CO)ʰ	1736	1741	1754	1752	1759

[a] Spectra run at 20 °C with δ in ppm, J in Hz, and ν in cm⁻¹. [b] Singlet resonances. [c] Septet resonances. [d] ³J(PtPᵈ). [e] ¹J(PtPᵈ). [f] ²J(PᵃC) = 9 Hz. [g] ²J(PᵈC) = 57 Hz. [h] 2 and 3e have ν(CO) = 1730 and 1729 cm⁻¹.

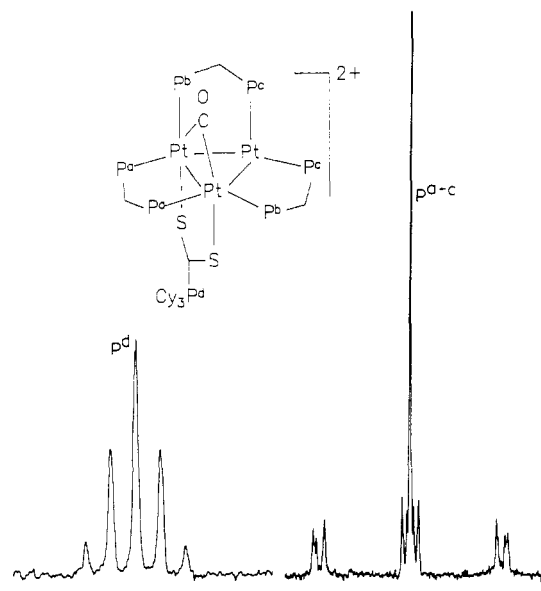Pt(3)-P(5) distances in both **2** and **3a**.

The asymmetric disposition of the carbonyl ligand with respect to the Pt₃ plane in **3a** is of particular interest in the light of recent theoretical work.[10] The CO ligand is strongly and symmetrically attached to Pt(1) and Pt(3) (Pt–C bond lengths 2.011 (11) and 2.023 (11) Å), whereas its contact with Pt(2) (2.67 (1) Å) can at most represent an extremely weak interaction. Comparison of the structural and spectroscopic parameters of the Pt₃(μ-CO) groups in **1**, **2**, and **3a** (Table II) suggests that the carbonyl slips from a symmetrical μ₃ bonding mode in **1** to a doubly bridging mode in **2** and **3a**. The Pt(2)···C distance in **2** of 2.47 (1) Å may indicate that this interaction is somewhat more important than in **3a**, implying that anionic dithiocarbamate transfers more charge to the cluster than electroneutral dmpm. The slippage of the μ₃-CO ligand toward the more highly substituted platinum atom can be rationalized if the carbonyl acts largely as a π-acceptor, as has been indicated by the EHMO calculations of Evans.[10] The lengthening of the C–O distances in **2** and **3a**

(10) Sutin, K. A.; Kolis, J. W.; Mlekuz, M.; Bougeard, P.; Sayer, B. G.; Quilliam, M. A.; Faggiani, R.; Lock, C. J. L.; McGlinchey, M. J.; Jaouen, G. *Organometallics* **1987**, *6*, 439.

Figure 2. ^{31}P NMR spectrum (121 MHz) of complex **3d**. The 1:4:7:4:1 intensity ratio for the inner five lines of the P^d resonance (δ = 48.9 ppm, ^3J(PtP) = 166 Hz; a 1:12:49:84:49:12:1 septet is expected on the basis of the natural abundance of ^{195}Pt, but the outer lines are usually not observed) and the single resonance for P^a–P^c (δ = –26.9 ppm, ^1J(PtP) = 3180 Hz) are characteristic of complexes with apparent 3-fold symmetry.
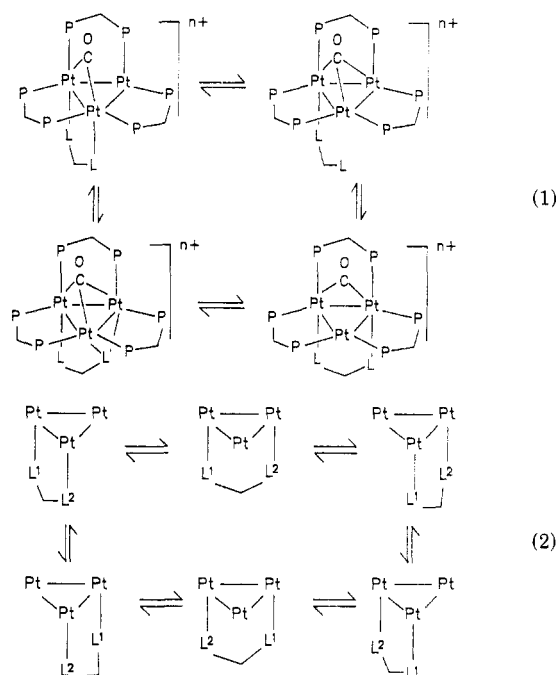
compared with those in **1** (Table II), though barely significant statistically, is consistent with this view. In addition, it should be noted that similar but smaller carbonyl slippages toward the more highly substituted metal atoms have been observed in the SCN$^-$ and P(OPh)$_3$ adducts of **1**.[2-4] Curiously, despite the greater asymmetry in the Pt$_3$(CO) bonding in **2** and **3a**, the Pt–Pt distances in these complexes show a range smaller than those in the more symmetrical μ_3-CO species **1** (see Table II).

Spectroscopic Properties and Fluxionality of Complexes 3a–f. The values for the ν(CO) stretching frequencies of **3** ranged from 1729 to 1759 cm^{-1} (Table III). All these frequencies are in the range expected for bridging carbonyl groups, and all are lower than the ν(CO) value of 1765 cm^{-1} observed for complex **1**.[1] These data, together with the trends in C–O bond distances discussed above, are consistent with there being stronger back-bonding to π^* orbitals of CO in **3** than in **1**, but the slippage of the CO ligand to the μ_2 bonding mode is a complicating factor.
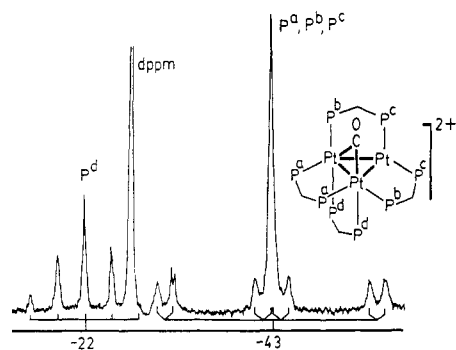
With the exception of **3e**, all complexes **3** were fluxional even at –90 °C, and spectral parameters obtained at room temperature in acetone-d_6 solution are reported in Table III. The fluxionality was easily identified by the ^{31}P{^{1}H} NMR spectra of **3a–d**, which contained only a singlet resonance, with platinum satellites, in each case, whereas three resonances due to P^a, P^b, and P^c are expected for the static structure. The spectra of complexes **3c** and **3d** contained another resonance at 54.4 and 48.9 ppm, respectively, due to the phosphorus atoms in the ligands Et$_3$PCS$_2$ and (C$_6$H$_{11}$)$_3$PCS$_2$. These resonances displayed the septet pattern, with the intensities of the inner five lines of the septet being 1:4:7:4:1 (Figure 2), characteristic of ligands that triply bridge three platinum centers.[2,5,7] This is also a clear indication of the fluxionality of these ligands about the triplatinum centers of **3c** and **3d**, since the static structure **3** would give different couplings to the nonequivalent platinum atoms. The presence of the averaged coupling to ^{195}Pt also shows that the R$_3$PCS$_2$ ligand does not fully dissociate from platinum during the fluxional process.

Complex **3f** was also fluxional, with the ^{31}P NMR spectrum containing two resonances in a 3:1 intensity ratio (Figure 3): the former is due to P^a, P^b, and P^c (equatorial dppm ligands; see Figure 2 for nomenclature), and the latter is due to P^d of the additional axial dppm ligand. The spectra were obtained in the presence of free dppm in order to prevent dissociation back to **1**, but the exchange between free and coordinated dppm was slow on the NMR time scale and did not seriously complicate the spectra (Figure 3). The resonance in the ^{31}P NMR spectrum due to P^d is particularly informative, in that it appears as a septet with the inner five lines having intensities 1:4:7:4:1 as expected if each phosphorus atom is in a Pt$_3$(μ_3-P) environment. The observed ^1J(PtP) value for this resonance is 720 Hz. If, as expected, the complex is fluxional and the coupling constant ^2J(PtP^d) is small, the true value for ^1J(PtP^d) is calculated to be $\sim 3 \times 720$ = 2160 Hz, which is close to the ^1J(PtP^d) value of 2592 Hz found for complex **2**. A mechanism of fluxionality involving complete dissociation of dppm is precluded by these NMR data, since such a mechanism would lead to a coalescence of resonances due to P^d and free dppm in addition to a loss of J(PtP^d) coupling. The dissociation of dppm from **3f** clearly can occur, since there is an equilibrium between **3f**, **1**, and free dppm, but this process must be much slower than the fluxional process. The fluxionality of **3f** could be frozen out at –124 °C in an acetone-d_6/CHCl$_2$F solvent mixture. Eight broad resonances were observed in addition to a singlet due to free dppm, and a plausible interpretation of these data is that steric interactions in [Pt$_3$(μ_3-CO)(μ-dppm)$_4$]$^{2+}$ (**3f**) are great enough to render each of the dppm phosphorus atoms inequivalent, giving eight sets of resonances instead of the expected four. The spectra were too poorly resolved to allow assignment of individual resonances.

The above data establish a common mechanism in which the added bidentate ligand can rotate about the Pt$_3$-(dppm)$_3$ triangle without dissociation. An intermediate with a monodentate ligand is possible, and there are many precedents for such species, but the data are also consistent with a concerted migration of donor atoms from one platinum to another, as shown in eq 1. There is no direct

$$(1)$$

$$(2)$$

precedent for a complex with a μ-PR$_3$ ligand, but evidence

Figure 3. ^{31}P NMR spectrum (121 MHz) of $[Pt_3(\mu\text{-}CO)(\mu\text{-}dppm)_4]^{2+}$ (**3f**) in the presence of free dppm (δ = -27 ppm). The upfield line of the 1:4:7:4:1 resonance due to P^d is obscured by the peak due to free dppm, but the intensities of the other four lines are characteristic. The predicted positions of ^{195}Pt satellites are given below the spectrum.

for such species as an intermediate or transition state has been obtained recently for PR_3 adducts of **1**.[3] Whichever of these mechanisms is correct, complete equivalence of platinum and ligand atoms requires six 60° rotations, as illustrated in eq 2. It is clear that the type of fluxionality shown in eqs 1 and 2 is possible only for coordinatively unsaturated clusters.

Complex **3e** was the only nonfluxional complex of those studied. The ^{31}P{^{1}H} NMR spectrum of **3e** consisted of four resonances of approximately equal intensity, and the resonances were assigned in a way similar to that described previously for complex **2**. We note that the data do not preclude a structure in which the dmpm and one dppm ligand of **3e** are interchanged and, if that were the case, it would not be necessary to assume nonfluxionality in order to interpret the ^{31}P NMR data.
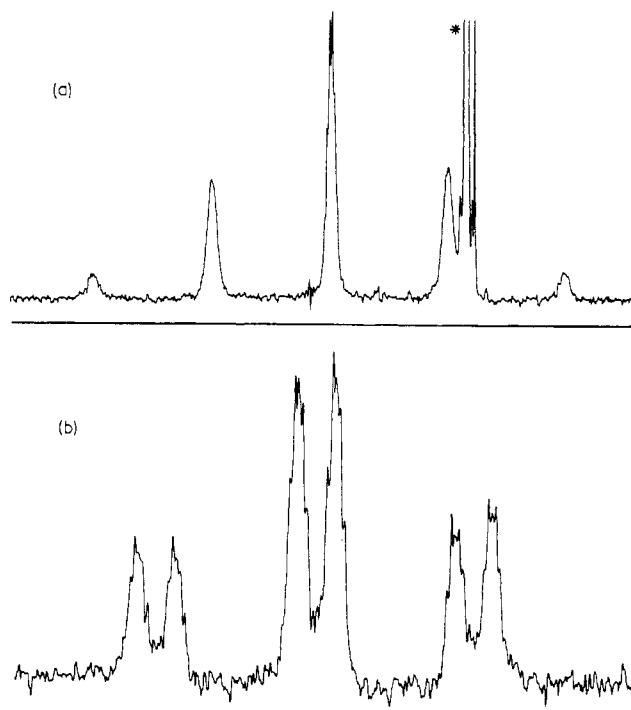
The ^{13}C{^{1}H} NMR spectra for the fluxional clusters **3a–d** and **3f** enriched with ^{13}CO consisted of septet resonances (Figure 4, only the inner five lines are observed) with chemical shifts ranging from 207.5 to 215.8 ppm and ^1J-(PtC) values ranging from 680 to 780 Hz. These parameters can be compared with those observed for the static cluster **3e**, where $\delta(^{13}$CO) = 219.1 ppm and ^1J(PtC) = 793 Hz. For **3a–d** and **3f** the apparent value of J(PtC) will be given by $^2/_3[^1J$(PtC)] + $^1/_3[^2J$(PtC)], as a result of the fast fluxionality, and so the values cannot be compared directly with that for the apparently static cluster **3e**.

The ^{1}H NMR spectra of **3a–d** and **3f** each contained an AB quartet due to the methylene protons of the μ-dppm ligands in the plane of the platinum triangle. These ligands appear to be equivalent because of the fluxionality, but this fluxional process does not create a plane of symmetry containing the $Pt_3(\mu\text{-}dppm)_3$ group, and so the $CH^AH^BP_2$ protons of each dppm ligand remain inequivalent.

The ^{195}Pt NMR spectrum of **3d** enriched with ^{13}CO (Figure 4) consisted of a doublet of triplets with δ = -2435 ppm, ^1J(PtP^{a,b,c}) = 3200 Hz (t), and ^1J(PtC) = 750 Hz (d). The coupling constants are within experimental error (±30 Hz) of the values obtained from the ^{31}P and ^{13}C NMR spectra. The observation of a single ^{195}Pt resonance is further proof of the fluxionality of the cluster (Figure 4). The spectrum of **3f**, on the other hand, consisted of a broad triplet at δ = -2887 ppm with ^1J(PtP^{a,b,c}) = 2900 Hz. Other couplings could not be determined due to the broadness of the resonance.

Discussion

This work has shown that bidentate ligands, LL, can add to the 42-electron cluster $[Pt_3(\mu_3\text{-}CO)(\mu\text{-}dppm)_3]^{2+}$ to give

Figure 4. (a) ^{13}CO NMR spectrum (75.6 MHz) of ^{13}CO-enriched of **3a**. The peak marked with an asterisk is due to solvent acetone-d_6, and the 1:4:7:4:1 intensity pattern of the five observed lines due to CO (δ = 207.5, ^1J(PtC) = 780 Hz) is characteristic of apparent 3-fold symmetry. (b) ^{195}Pt NMR spectrum (64 MHz) of ^{13}CO-enriched **3d** (δ = -2435 ppm). The triplet splitting is due to ^1J(PtP) = ca. 3200 Hz and the doublet to ^1J(PtC) = ca. 750 Hz. Long-range PtP couplings (<200 Hz) are not fully resolved.

the 46-electron clusters $[Pt_3(\mu\text{-}CO)(\mu\text{-}dppm)_3(\mu\text{-}LL)]^{n+}$. In these complexes, slippage of the carbonyl ligand from a μ_3 to a μ_2 bonding mode occurs, apparently because the carbonyl ligand acts primarily as an acceptor ligand and back-bonding is stronger from the platinum atoms with higher coordination number. There is some evidence for this enhanced back-bonding from the lower values of ν(CO) in **3** compared to those of **1** and also from the C–C bond lengths (Table II). An alternative interpretation of the bonding is to consider the compounds **3** to be formed from the fragments $[Pt_3(\mu\text{-}dppm)_3(LL)]$ and CO^{2+}. The CO^{2+} ligand acts as both a σ- and π-acceptor ligand and so naturally adds to the platinum centers with higher electron density. The difference between the two interpretations is that the second does not *require* a π-acceptor ligand, and a similar slippage would then also be expected for ligands, such as H^+, that are σ-acceptors only.

The remarkably easy fluxionality of most complexes **3** is a result of the coordinative unsaturation, which allows easy migration of a ligand between platinum centers. Normally, phosphorus and sulfur donors do not undergo this type of fluxionality, and we know of no direct precedents. Monodentate phosphorus donors undergo a related fluxionality in the complexes $[Pt_3(\mu_3\text{-}CO)(PR_3)(\mu\text{-}dppm)_3]^{2+}$, in which a transition state with a μ_3-PR_3 group was proposed.[2,3] The arsenic donor in the ligand $Ph_2PCH_2CH_2AsPh_2$ can migrate between metal centers by a dissociative mechanism, and $[Ag_2(\mu\text{-}dppm)_3]^{2+}$ undergoes easy end-to-end exchange of the μ-dppm ligands.[10,11]

One puzzling aspect of this work is why the dmpm complexes **2** and **3e** are not fluxional. Perhaps the ligand

(11) Dean, P. A. W.; Vittal, J. J.; Srivastava, R. S. *Can. J. Chem.* **1987**, *65*, 2628.

Table IV. Fractional Atomic Coordinates and Thermal Parameters for [Pt$_3$(μ-CO)(μ-dppm)$_3$(μ-S$_2$CNMe$_2$)][PF$_6$] (3a[PF$_6$])

	x/a	y/b	z/c	U,^{a} Å^2		x/a	y/b	z/c	U,^{a} Å^2
Pt(1)	0.30328 (2)	-0.23601 (3)	-0.12626 (1)	0.028	C(D6)	0.3409 (5)	-0.1219 (7)	-0.3273 (5)	0.058 (3)
Pt(2)	0.24238 (2)	-0.12841 (3)	-0.19044 (1)	0.029	C(E1)	0.1743 (6)	0.0950 (6)	-0.2205 (4)	0.036 (3)
Pt(3)	0.17035 (2)	-0.21360 (3)	-0.12533 (1)	0.027	C(E2)	0.1822 (7)	0.1521 (9)	-0.2604 (3)	0.065 (4)
S(1)	0.32803 (13)	-0.08617 (23)	-0.07958 (10)	0.043	C(E3)	0.1969 (4)	0.2505 (7)	-0.2559 (3)	0.079 (4)
S(2)	0.17351 (13)	-0.05513 (22)	-0.08085 (13)	0.040	C(E4)	0.2035 (5)	0.2918 (5)	-0.2115 (3)	0.079 (4)
P(1)	0.39886 (13)	-0.26247 (22)	-0.17095 (10)	0.035	C(E5)	0.1956 (6)	0.2347 (8)	-0.1716 (2)	0.060 (4)
P(2)	0.33917 (13)	-0.09260 (22)	-0.22866 (9)	0.032	C(E6)	0.1809 (3)	0.1363 (7)	-0.1761 (3)	0.046 (3)
P(3)	0.15871 (13)	-0.03796 (21)	-0.22327 (10)	0.034	C(F1)	0.1303 (6)	-0.0600 (10)	-0.2843 (2)	0.038 (3)
P(4)	0.07265 (12)	-0.18084 (21)	-0.16901 (9)	0.031	C(F2)	0.0745 (7)	-0.0117 (5)	-0.3033 (4)	0.050 (4)
P(5)	0.15349 (13)	-0.28968 (21)	-0.5147 (9)	0.033	C(F3)	0.0505 (3)	-0.363 (8)	-0.3479 (4)	0.062 (4)
P(6)	0.30893 (13)	-0.32700 (22)	-0.05547 (9)	0.033	C(F4)	0.0823 (5)	-0.1091 (8)	-0.3734 (2)	0.063 (4)
P(7)	0.72740 (14)	0.40578 (27)	0.36422 (12)	0.081	C(F5)	0.1381 (5)	-0.1574 (4)	-0.3543 (4)	0.062 (4)
F(1)	0.8054 (2)	0.4080 (7)	0.3614 (3)	0.131	C(F6)	0.1621 (3)	-0.1328 (10)	-0.3097 (4)	0.043 (3)
F(2)	0.6494 (2)	0.4036 (7)	0.3671 (3)	0.202	C(G1)	0.0540 (7)	-0.2467 (9)	-0.2238 (2)	0.035 (3)
F(3)	0.7307 (6)	0.4664 (7)	0.4097 (2)	0.166	C(G2)	0.0014 (6)	-0.2141 (4)	-0.2526 (4)	0.043 (3)
F(4)	0.7240 (6)	0.3452 (7)	0.3187 (2)	0.162	C(G3)	-0.0130 (3)	-0.2616 (9)	-0.2947 (4)	0.054 (3)
F(5)	0.7314 (2)	0.3116 (5)	0.3935 (3)	0.117	C(G4)	0.0252 (6)	-0.3417 (8)	-0.3080 (2)	0.060 (3)
F(6)	0.7234 (2)	0.4999 (5)	0.3350 (3)	0.154	C(G5)	0.0778 (5)	-0.3743 (6)	-0.2791 (4)	0.062 (4)
O	0.2245 (3)	-0.3876 (6)	-0.1822 (3)	0.045 (2)	C(G6)	0.0922 (4)	-0.3268 (10)	-0.2371 (4)	0.052 (3)
N	0.2627 (4)	0.0438 (7)	-0.312 (3)	0.049 (3)	C(H1)	-0.0129 (4)	-0.187 (7)	-0.1424 (4)	0.040 (3)
C(1)	0.3886 (5)	-0.2068 (8)	-0.2298 (4)	0.043 (3)	C(H2)	-0.511 (5)	-0.1057 (6)	-0.1310 (2)	0.056 (3)
C(2)	0.0797 (5)	-0.0522 (8)	-0.1893 (4)	0.037 (3)	C(H3)	-0.1163 (5)	-0.1168 (5)	-0.1137 (4)	0.077 (4)
C(3)	0.2362 (5)	-0.2876 (8)	-0.0200 (4)	0.041 (3)	C(H4)	-0.1432 (3)	-0.2092 (6)	-0.1078 (3)	0.069 (4)
C(4)	0.2550 (5)	-0.0262 (8)	-0.0625 (4)	0.038 (3)	C(H5)	-0.1051 (5)	-0.2906 (5)	-0.1191 (3)	0.059 (4)
C(5)	0.3295 (6)	0.0714 (10)	-0.0106 (4)	0.065 (4)	C(H6)	-0.0399 (6)	-0.2796 (6)	-0.1364 (5)	0.049 (3)
C(6)	0.2043 (6)	0.0955 (11)	-0.0118 (5)	0.071 (4)	C(I1)	0.0969 (6)	-0.2270 (4)	-0.102 (5)	0.037 (3)
C(7)	0.2291 (5)	-0.3121 (8)	-0.1596 (4)	0.041 (3)	C(I2)	0.0301 (7)	-0.2146 (9)	-0.251 (3)	0.054 (3)
C(A1)	0.4145 (6)	-0.3908 (4)	-0.1856 (4)	0.040 (3)	C(I3)	-0.0145 (4)	-0.1606 (10)	0.0018 (4)	0.068 (4)
C(A2)	0.4638 (6)	-0.4423 (10)	-0.1607 (2)	0.055 (3)	C(I4)	0.0076 (5)	-0.1189 (4)	0.0438 (4)	0.061 (4)
C(A3)	0.4699 (3)	-0.5421 (10)	-0.1669 (4)	0.068 (4)	C(I5)	0.0744 (6)	-0.1313 (9)	0.0588 (2)	0.071 (4)
C(A4)	0.4267 (5)	-0.5904 (4)	-0.1981 (4)	0.065 (4)	C(I6)	0.1190 (3)	-0.1854 (10)	0.0318 (4)	0.056 (3)
C(A5)	0.3775 (5)	-0.5388 (10)	-0.2230 (2)	0.072 (4)	C(J1)	0.1258 (6)	-0.4172 (6)	-0.0493 (4)	0.043 (3)
C(A6)	0.3714 (3)	-0.4390 (10)	-0.2167 (5)	0.060 (4)	C(J2)	0.1240 (3)	0.4728 (7)	-0.0900 (4)	0.051 (3)
C(B1)	0.4821 (5)	-0.2182 (11)	-0.1496 (4)	0.046 (3)	C(J3)	0.1045 (6)	-0.5698 (9)	-0.0881 (3)	0.071 (4)
C(B2)	0.5381 (7)	-0.2215 (11)	-0.1787 (3)	0.067 (4)	C(J4)	0.0869 (5)	-0.6112 (5)	-0.0454 (4)	0.085 (5)
C(B3)	0.5998 (5)	-0.1837 (4)	-0.1634 (4)	0.078 (4)	C(J5)	0.0887 (4)	-0.5556 (8)	-0.0046 (2)	0.102 (5)
C(B4)	0.6056 (5)	-0.1429 (10)	-0.1188 (3)	0.084 (5)	C(J6)	0.1082 (7)	-0.4586 (9)	-0.0065 (4)	0.075 (4)
C(B5)	0.5496 (7)	-0.1396 (8)	-0.0897 (3)	0.095 (5)	C(K1)	0.3024 (6)	-0.4614 (5)	-0.0569 (4)	0.040 (3)
C(B6)	0.4878 (4)	-0.1772 (6)	-0.1051 (4)	0.060 (3)	C(K2)	0.3123 (3)	-0.5090 (7)	-0.0994 (3)	0.050 (3)
C(C1)	0.3930 (6)	-0.0004 (8)	-0.2014 (2)	0.036 (3)	C(K3)	0.3091 (6)	-0.6098 (7)	-0.1014 (3)	0.058 (3)
C(C2)	0.4623 (7)	0.0054 (5)	-0.2095 (4)	0.051 (4)	C(K4)	0.2961 (5)	-0.6631 (4)	-0.0610 (4)	0.078 (4)
C(C3)	0.5005 (3)	0.0790 (7)	-0.1888 (4)	0.059 (3)	C(K5)	0.2862 (4)	-0.6155 (7)	-0.0186 (2)	0.081 (4)
C(C4)	0.4694 (5)	0.1470 (7)	-0.1600 (2)	0.055 (3)	C(K6)	0.2893 (7)	-0.5147 (8)	-0.0165 (4)	0.066 (4)
C(C5)	0.4001 (6)	0.1413 (4)	-0.1519 (4)	0.068 (4)	C(L1)	0.3833 (5)	-0.3097 (12)	-0.0159 (4)	0.039 (3)
C(C6)	0.3620 (3)	0.0676 (8)	-0.1726 (3)	0.049 (3)	C(L2)	0.3861 (4)	-0.2347 (8)	0.0167 (5)	0.050 (3)
C(D1)	0.3371 (5)	-0.0551 (11)	-0.2908 (4)	0.041 (3)	C(L3)	0.4452 (7)	-0.2188 (7)	0.0427 (4)	0.070 (4)
C(D2)	0.3321 (7)	0.0436 (10)	-0.3007 (4)	0.065 (4)	C(L4)	0.5014 (4)	-0.2780 (10)	0.0360 (3)	0.076 (4)
C(D3)	0.3310 (5)	0.0754 (8)	-0.3471 (5)	0.112 (6)	C(L5)	0.4985 (5)	-0.3531 (6)	0.0034 (5)	0.075 (4)
C(D4)	0.3348 (4)	0.0085 (9)	-0.3836 (3)	0.098 (5)	C(L6)	0.4394 (7)	-0.3689 (9)	-0.0226 (3)	0.060 (3)
C(D5)	0.3398 (7)	-0.0902 (8)	-0.3737 (4)	0.087 (5)					

^{a} For Pt, S, P, and F atoms U is one-third of the trace of the orthogonalized U_{ij} tensor. For the other atoms it defines the isotropic temperature factor $\exp(-8\pi^2 U(\sin^2 \theta)/\lambda^2)$.

dmpm binds too strongly for easy fluxionality (eq 1). The ligand dppm evidently binds more weakly in **3f** due to steric effects, and it is remarkable that the fluxionality occurs so easily in such a sterically congested molecule.

Experimental Section

^{1}H NMR spectra were recorded by using a Varian XL-200 spectrometer, and ^{31}P{^{1}H}, ^{13}C{^{1}H}, and ^{195}Pt{^{1}H} NMR spectra were recorded by using a Varian XL-300 spectrometer. ^{1}H and ^{13}C chemical shifts were measured relative to Me$_4$Si; ^{31}P and ^{195}Pt chemical shifts were measured relative to 85% H$_3$PO$_4$ and aqueous K$_2$PtCl$_4$, respectively. The solvent used in all cases was acetone-d_6 unless otherwise noted. Infrared spectra, usually as Nujol mulls, were recorded on a Bruker IR/32 FT-IR spectrometer equipped with an IBM 9000 computer.

[Pt$_3$(μ-CO)(μ-dppm)$_3$(μ_2-S$_2$CNMe$_2$)][PF$_6$] (3a[PF$_6$]). (C-H$_3$)$_2$NCS$_2$Na·2H$_2$O (3.5 mg) was added to complex 1 (40 mg) dissolved in acetone (10 mL). The mixture was stirred until all of the ligand had dissolved, the solvent was removed, and the solid product, as the water solvate, was washed with water (3 × 10 mL) and dried in vacuo. Anal. Calcd for C$_{79}$H$_{72}$NOS$_2$F$_6$P$_7$Pt$_3$·4H$_2$O:

C, 45.1; H, 3.8; N, 0.7. Found: C, 44.7; H, 3.4; N, 0.6. IR: ν(CO) 1736 cm^{-1}, ν(CS) 1102 cm^{-1}, ν(OH) 3500 (br) cm^{-1}. ^{1}H NMR (δ): 3.83 [s, CH$_3$]; 5.24, 5.70 [AB, CH$_2$P$_2$]. It was recrystallized from acetone/pentane to give red crystals of the acetone solvate.

[Pt$_3$(μ-CO)(μ-dppm)$_3$(μ-S$_2$CN(CH$_2$CH$_3$)$_2$)][PF$_6$] (3b[PF$_6$]). This was prepared in a similar way from (C$_2$H$_5$)$_2$NCS$_2$Na·3H$_2$O (4.4 mg) and complex 1 (40 mg) in acetone (10 mL). Anal. Calcd for C$_{81}$H$_{76}$NOS$_2$F$_6$P$_7$Pt$_3$·4H$_2$O: C, 45.6; H, 4.0; N, 0.7. Found: C, 45.2; H, 3.8; N, 0.9. IR: ν(CO) 1741 cm^{-1}, ν(CS) 1098 cm^{-1}, ν(OH) 3500 cm^{-1} (br). ^{1}H NMR (δ): 1.61 [q, ^3J(HH) = 8 Hz, CH$_2$CH$_3$]; 4.32 [t, CH$_2$CH$_3$]; 5.23, 5.70 [AB, ^2J(HH) = 16 Hz].

[Pt$_3$(μ-CO)(μ-dppm)$_3$(μ-S$_2$CP(C$_2$H$_5$)$_3$)][PF$_6$]$_2$ (3c[PF$_6$]$_2$). (C$_2$H$_5$)$_3$PCS$_2$ (3.8 mg) was added to a solution of complex 1 (40 mg) in acetone (10 mL). Reaction occurred instantly, and the product was isolated as above. Anal. Calcd for C$_{83}$H$_8$OS$_2$F$_{12}$P$_9$Pt$_3$: C, 44.3; H, 3.6. Found: C, 44.6; H, 3.8. IR: ν(CO) 1754 cm^{-1}. ^{1}H NMR (δ): 2.73 [d/q, ^2J(PH) = 14 Hz, CH$_2$CH$_3$P]; 1.17 [d/t, ^3J(PH) = 18 Hz, ^3J(HH) = 14 Hz]; 5.38 [br, CH$_2$P$_2$].

[Pt$_3$(μ-CO)(μ-dppm)$_3$(μ-S$_2$CP(C$_6$H$_{11}$)$_3$)][PF$_6$]$_2$ (3d[PF$_6$]$_2$). This was prepared in a similar way from (C$_6$H$_{11}$)$_3$PCS$_2$ (7 mg) and complex 1 (40 mg) in acetone (10 mL). Anal. Calcd for

$C_{95}H_{99}OS_2F_{12}P_9Pt_3$: C, 47.3; H, 4.1. Found: C, 47.7; H, 4.4. IR: ν(CO) 1752 cm⁻¹.

[Pt₃(μ-CO)(μ-dppm)₃(μ-dmpm)][PF₆]₂ (3e[PF₆]₂). dmpm (3.6 μL) was added to a solution of complex 1 (40 mg) in acetone (10 mL). Reaction was instantaneous, with the solution changing from orange-red to red-black. The product was isolated as above. Anal. Calcd for $C_{81}H_{80}OF_{12}P_{10}Pt_3$: C, 43.5; H, 3.7. Found: C, 43.5; H, 4.1. IR: ν(CO) 1729 cm⁻¹. ¹H NMR (δ): 4.85, 2.27 [br, CH₂P₂]. ¹³C NMR (δ): 219.1 [m, ¹J(PtC) = 793 Hz, ²J(PᵈC) = 57 Hz, CO). ³¹P NMR (δ): -25.5 [m, ¹J(PtP) = 3265 Hz, ³J(PᵃPᶜ) = 215 Hz, Pᵃ]; -61.5 [m, ¹J(PtP) = 3060 Hz, ³J(PᵇPᵇ′) = 205 Hz, Pᵇ]; -39.0 [m, ¹J(PtP) = 2140 Hz, ³J(PᵃPᶜ) = 215 Hz, Pᶜ]; -46.0 [m, ¹J(PtP) = 2070 Hz, ³J(PᵈPᵈ′) = 205 Hz, Pᵈ].

[Pt₃(μ-CO)(μ-dppm)₄][PF₆]₂ (3f[PF₆]₂). dppm (15 mg) was added to complex 1 (40 mg) in acetone (10 mL). This corresponds to a 2-fold excess of ligand to cluster. Reaction occurred immediately, and pure 3f was isolated by cooling the solution to 0 °C to allow crystallization to occur. The black crystals of 3f were then separated by hand from the red crystals of 1 that also formed. The product was dried in vacuo. Anal. Calcd for $C_{101}H_{88}OF_{12}P_{10}Pt_3$: C, 49.7; H, 3.6. Found: C, 49.7; H, 3.8. IR: ν(CO) 1759 cm⁻¹. ¹H NMR (δ): 6.26, 5.68 [AB, CH₂P₂]. ³¹P NMR (-124 °C, δ): -8.81 [m, ¹J(PtP) = 2440 Hz, ³J(PP) = 220 Hz]; -34.23 [m, ¹J(PtP) = 3160 Hz]; -36.22 [m, ¹J(PtP) = 2180 Hz, ³J(PP) = 210 Hz]; -38.04 [m, ¹J(PtP) = 3008 Hz, ³J(PP) = 240 Hz]; -40.03 [br]; -51.12 [m, ¹J(PtP) = 3560 Hz, ³J(PP) = 220 Hz]; -54.10 [m, ¹J(PtP) = 1520 Hz, ³J(PtP) = 220 Hz]; -78.66 [m, ¹J(PtP) = 2920 Hz, ¹J(PtP) = 200] Hz]; the peaks were broad, and J values are ±10 Hz.

X-ray Analysis of [Pt₃(μ-CO)(μ-dppm)₃(μ-S₂CNMe₂)][PF₆] (3a[PF₆]). Crystal Data. $C_{79}H_{72}F_6NOP_7Pt_3S_2$, fw = 2031.7, monoclinic, space group $P2_1/c$, a = 19.583 (3) Å, b = 13.661 (3) Å, c = 28.245 (5) Å, β = 90.64 (2)°, V = 7556 (2) Å³, Z = 4, d(calcd) = 1.786 g cm⁻³, λ(Mo Kα) = 0.710 69 Å, μ(Mo Kα) = 58.6 cm⁻¹, F(000) = 3944, T = 22 °C.

Measurements. A purple crystal of dimensions 0.84 × 0.72 × 0.72 mm was used. All measurements were made with Mo X-rays on an Enraf-Nonius CAD4F diffractometer fitted with a graphite monochromator. Cell dimensions were obtained from the setting angles of 23 reflections with 12 < θ(Mo Kα) < 14°. The intensities of 12048 reflections with 2 < θ(Mo Kα) < 22° (h, 0-20; k, $\overline{14}$-3; l, $\overline{29}$-29) were obtained from $\omega/2\theta$ scans of 0.80°

in θ, extended by ¹/₄ at each end to estimate background. The intensities of two standard reflections showed only random fluctuations of up to 5% about their mean values during the experiment. After correction for absorption by an empirical method[12] (transmission factors on F 0.87-1.20) and averaging of 2684 duplicate measurements (R_{int} = 0.039) 9218 unique intensities were obtained, of which 6699 with $I > 3\sigma(I)$ were used in subsequent calculations.

Structure Analysis. The structure was solved by Patterson and difference Fourier methods. In the final full-matrix least-squares refinement on F, with $w^{-1} = \sigma^2(F) + 0.00023F^2$, anisotropic U_{ij} values were refined only for Pt, S, P, and F atoms. The [PF₆]⁻ anion was treated as a rigid group (P-F = 1.53 Å, F-P-F = 90 or 180°), as were the 12 C₆H₅ rings (C-C = 1.38 Å, C-H = 0.96 Å, C-C-C = 120°). Methyl and methylene H atoms were constrained to ride on their parent C atoms with C-H = 0.96 Å and U(H) = 1.2[U(C)], methyl group orientations being initially obtained from difference syntheses. Adjustment of 328 parameters converged (maximum shift/esd ratio <0.03) at R = 0.033 and R_w = 0.044. The final difference synthesis was featureless ($\Delta\rho$ < 1.0 e Å⁻³), and the mean $w\Delta^2$ value showed no systematic variation with F or (sin θ)/λ. Scattering factors for neutral atoms and anomalous dispersion corrections were taken from ref 13. All calculations were performed with the local GX package[14] on a Gould 32/27 minicomputer. Final parameters for non-hydrogen atoms are presented in Table IV.

(12) Walker, N.; Stuart, D. *Acta Crystallogr., Sect. A: Found. Crystallogr.* **1983**, *A39*, 158.

(13) *International Tables of X-ray Crystallography*; Kynoch: Birmingham, England, 1974; Vol. IV, pp 99, 149.

(14) Mallinson, P. R.; Muir, K. W. *J. Appl. Crystallogr.* **1985**, *18*, 51.